Article No. jmbi.1999.3388 available online at http://www.idealibrary.com on IDEAL® J. Mol. Biol. (2000) 295, 1129–1137

JMB

COMMUNICATION

Hydration of [d(CGC)r(aaa)d(TTTGCG)]$_2$

Shang-Te Hsu[1], Mei-Tsen Chou[1], Shan-Ho Chou[2], Wen-Chang Huang[3] and Jya-Wei Cheng[1]*

[1]*Division of Structural Biology and Biomedical Science Department of Life Science National Tsing Hua University Hsinchu 300, Taiwan, ROC*

[2]*Institute of Biochemistry National Chung Hsing University, Taichung 400 Taiwan, ROC*

[3]*Department of Chemistry Taiwan Normal University Taipei, Taiwan, ROC*

**Corresponding author*

We have studied the hydration and dynamics of RNA C2′-OH in a DNA·RNA hybrid chimeric duplex [d(CGC)r(aaa)d(TTTGCG)]$_2$. Long-lived water molecules with correlation time τ_c larger than 0.3 ns were found close to the RNA adenine H2 and H1′ protons in the hybrid segment. A possible long-lived water molecule was also detected close to the methyl group of 7T in the RNA-DNA junction but not to the other two thymine bases (8T and 9T). This result correlates with the structural studies that only DNA residue 7T in the RNA-DNA junction adopts an O4′-*endo* sugar conformation (intermediate between *B*-form and *A*-form), while the other DNA residues including 3C in the DNA-RNA junction, adopt C1′-*exo* or C2′-*endo* conformations (in the *B*-form domain). Based on the NOE cross-peak patterns, we have found that RNA C2′-OH tends to orient toward the O3′ direction, forming a possible hydrogen bond with the 3′-phosphate group. The exchange rates for RNA C2′-OH were found to be around 5-20 s^{-1}, compared to 26.7(±13.8) s^{-1} reported previously for the other DNA·RNA hybrid duplex. This slow exchange rate may be due to the narrow minor groove width of [d(CGC)r(aaa)d(TTTGCG)]$_2$, which may trap the water molecules and restrict the dynamic motion of hydroxyl protons. The distinct hydration patterns of the RNA adenine H2 and H1′ protons and the DNA 7T methyl group in the hybrid segment, as well as the orientation and dynamics of the RNA C2′-OH protons, may provide a molecular basis for further understanding the structure and recognition of DNA·RNA hybrid and chimeric duplexes.

Keywords: NMR spectroscopy; DNA·RNA hybrid hydration; water residence time; C2′-OH exchange rate; C2′-OH orientation

The structure and recognition of DNA·RNA hybrid and chimeric duplexes have been the focus of numerous studies because of their crucial roles in transcription, reverse transcription, and replication (Arnott *et al*., 1986; Chou *et al*., 1989; Cross *et al*., 1997; Fedoroff *et al*., 1997; Gao & Jeffs, 1994; Gmeiner *et al*., 1990; Gonzalez *et al*., 1994, 1995; Gyi *et al*., 1966, 1998b; Hashem *et al*., 1998; Katahira *et al*., 1990; Lane *et al*., 1993; Maltseva *et al*., 1994; Mujeeb *et al*., 1997; Rice & Gao, 1997; Salazar *et al*., 1993b; Steely *et al*., 1986). The NMR structural studies of DNA·RNA hybrid duplexes have revealed that they adopt neither an *A*-form nor a *B*-form structure in solution, but an intermediate heteromerous duplex structure (Chou *et al*., 1991; Salazar *et al*., 1993b). The sugars of the RNA strand have the normal N-type C3′-*endo* conformation, but those of the DNA strand have an intermediate O4′-*endo* conformation or have multiple conformers in dynamic exchange (Chou *et al*., 1991; Gonzalez *et al*., 1994, 1995; Gyi *et al*., 1998b). The minor groove width of DNA·RNA hybrid duplexes was found to be between that of the *A*- and *B*-form duplex values (Fedoroff *et al*., 1993). These structural features were used to explain the mechanism whereby RNase H discriminates between DNA·RNA hybrid duplexes and pure RNA or DNA duplexes (Fedoroff *et al*., 1993).

The X-ray crystallographic studies have found that even the introduction of one ribonucleotide into the DNA strand transforms the whole duplex to the *A*-form geometry with all the sugars in the C3′-*endo* conformation (Ban *et al*., 1994a,b; Egli *et al*.,

E-mail address of the corresponding author: lscjw@life,nthu.edu.tw

0022-2836/00/51129–9 $35.00/0

1993). Similar results have been reported for the structures of several Okazaki fragments determined by X-ray crystallography (Egli *et al*., 1993; Wang *et al*., 1982). On the other hand, NMR studies have revealed that for Okazaki fragments, the DNA·RNA hybrid section assumes a conformation similar to that found for pure hybrid duplexes, while the DNA section assumes a conformation closer to *B*-form DNA (Fedoroff *et al*., 1996; Nishizaki *et al*., 1996; Salazar *et al*., 1993a, 1994, 1996). When one ribonucleotide was inserted into the DNA strand, the overall conformation of this chimeric duplex was found to remain as *B*-form DNA, except that the sugar pucker of the RNA was switched to the C3′-*endo* conformation (Jaishree *et al*., 1993). When a DNA duplex is flanked by DNA·RNA hybrids, the central DNA fragment was again found to adopt a *B*-form conformation and the transition from *A*-form RNA to *B*-form DNA involves only one nucleotide step (Zhu *et al*., 1995).

The differences between X-ray crystallographic and NMR studies regarding the conformations of DNA·RNA hybrid and chimeric duplexes may arise from the presence of water molecules. Water has been found to play an important role in nucleic acid structure and recognition, as dehydration of DNA causes its conformation to change from *B*-form into the *A*-form (Saenger, 1984). In contrast, RNA is found locked in the *A*-form conformation in both the crystal and solution states (Saenger, 1984). Water is also reported to be involved in both the specificity and affinity of protein-DNA interactions (Billeter *et al*., 1996; Morton & Ladbury, 1996; Schwabe, 1997). Recently, it has been proposed that RT-associated RNaseH domain, which degrades the RNA template of DNA·RNA hybrid chimeric duplexes, may distinguish double-stranded RNA, RNA·DNA junctions and hybrid duplexes according to their distinct hydration patterns (Szyperski *et al*., 1999). Although several X-ray and NMR analyses of DNA (Berman, 1994; Denisov *et al*., 1997; Drew & Dickerson, 1981; Fawthrop *et al*., 1993; Guerri *et al*., 1998; Jacobson *et al*., 1996; Johannesson & Halle, 1998; Kubinec & Wemmer, 1992; Lane *et al*., 1997; Liepinsh *et al*., 1992, 1994; Phan *et al*., 1999; Prive *et al*., 1987; Quintana *et al*., 1992; Sunnerhagen *et al*., 1998; Zhou & Bryant, 1996) and RNA (Conte *et al*., 1996; Gyi *et al*., 1998a) hydration have appeared, little is known about the hydration of DNA·RNA hybrid and chimeric duplexes. The possible correlation between structure and function of DNA·RNA hybrid and chimeric duplexes and their interactions with important enzymes, such as HIV reverse transcriptase and RNase H, prompted us o study the hydration of a chimeric duplex $[d(CGC)r(aaa)d(TTTGCG)]_2$, in which the hybrid junctions are flanked by DNA duplexes at both ends.

Hydration of $[d(CGC)r(aaa)d(TTTGCG)]_2$

The d(CGC)r(aaa)d(TTTGCG) dodecamer was synthesized on a DNA synthesizer (Applied Biosystems 380B) using solid-phase phosphoramidite chemistry, as described (Chou *et al*., 1989, 1991). The sample was then purified by C-18 reversed-phase HPLC followed by DEAE ion-exchange column chromatography and desalted on a Sephadex G-10 column. The purified sample (15 mg) was freeze-dried and was dissolved in 0.3 ml of 90% H_2O, 10 % ^2H_2O containing 20 mM sodium phosphate, 200 mM sodium chloride and 0.05 mM EDTA, pH 7.0.

All spectra were carried out at 14.1 T on a Bruker AVANCE 600 MHz spectrometer. Phase sensitive NOESY and ROESY spectra were recorded at 273, 278, 283 and 300 K under identical conditions, except for their different mixing time of 100 and 50 ms, respectively. The intense bulky water signal was suppressed using the Watergate method (Piotto *et al*., 1992) with a short delay τ of 139 μs, resulting in the optimum excitation near 1.7, 7.7, and 13.7 ppm. These spectra were collected into 2048 complex points in the t_2 dimension and 800 complex points in the t_1 dimension with a relaxation delay of 1.4 seconds between each scan. The data were further apodized with a sine-square window function and zero-filled to 4096 complex points in the t_2 dimension and 1024 complex points in the t_1 dimension. After Fourier transformation, the data were phased by the TPPI method and treated with base-line correction along both dimensions to yield pure absorptive spectra.

The qualitative and quantitative water hydration residence time was determined by the cross-relaxation rate constants of the laboratory frame NOE and the rotating frame ROE. The cross-relaxation rate constants of NOE and ROE are given by (Otting *et al*., 1991):

$$\sigma^{NOE} = (\alpha/r^6)[6J(2\omega) - J(0)]$$
$$\sigma^{ROE} = (\alpha/r^6)[3J(\omega) + 2J(0)] \quad (1)$$

where α is a constant, and $J(\omega)$ is the spectral density function. When the local motion is neglected and the relaxation is dominated mainly by rotation, the spectral density function is simplified to a function of both Larmor frequency ω and correlation τ_c:

$$J(\omega) = \tau_c/(1 + \omega^2\tau_c^2) \quad (2)$$

Equation (1) shows that, σ^{ROE} is always positive, while σ^{NOE} changes its sign when $\omega\tau_c = 1.12$ (i.e. $\tau_c = 0.3$ ns under 14.1 T). Hence, by defining the ratio $R = \sigma^{NOE}/\sigma^{ROE}$, we can determine the water residence time. When the water residence time is long ($\omega\tau_c > 0.3$ ns), we should be able to observe cross-peaks with opposite signs in the NOESY (positive) and ROESY (negative) spectra.

Experimentally, we can determine the ratio R by integrating the cross-peak volumes in NOESY

(I^{NOESY}) and ROESY (I^{ROESY}) spectra:

$$R_{exp} = I^{NOESY}/I^{ROESY} \quad (3)$$

Using the cytosine H5/H6 cross-peak as an internal standard, we can eliminate the effect of Watergate terms between NOESY and ROESY spectra, which gives a simple equation (Lane *et al.*, 1997):

$$R_{exp} = -2[\sigma^{NOE}/\sigma^{NOE}] = -2R \quad (4)$$

Figure 1 shows the expanded region of the 2D NOESY spectrum of $[d(CGC)r(aaa)d(TTTGCG)]_2$ in H_2O recorded at 278 K, 14.1 T. The exchangeable and non-exchangeable proton cross-peaks of $[d(CGC)r(aaa)d(TTTGCG)]_2$ were assigned using NOESY, ROESY, and TOCSY spectra. The H1′ protons were assigned by the standard sequential assignment method, followed by assignment of the H2′ and H2″ protons of DNA, as well as the H3′ and H4′ protons of all residues (Hare *et al.*, 1983; Wuthrich, 1986). The H2′ protons of the three RNA adenine bases were assigned using the H2′-H3′ cross-peaks of the TOCSY spectrum. All three RNA adenine H2 protons showed both interresidue and intraresidue cross-peaks, particularly in the H6/H8-H1′ region (Figure 1). The cross-peaks between RNA adenine H2 protons and water along the *F*2 dimension were clearly identified, except for the overlapped cross-peak of 4a H2, which was buried in the intense cross-peaks of hydroxyl protons.

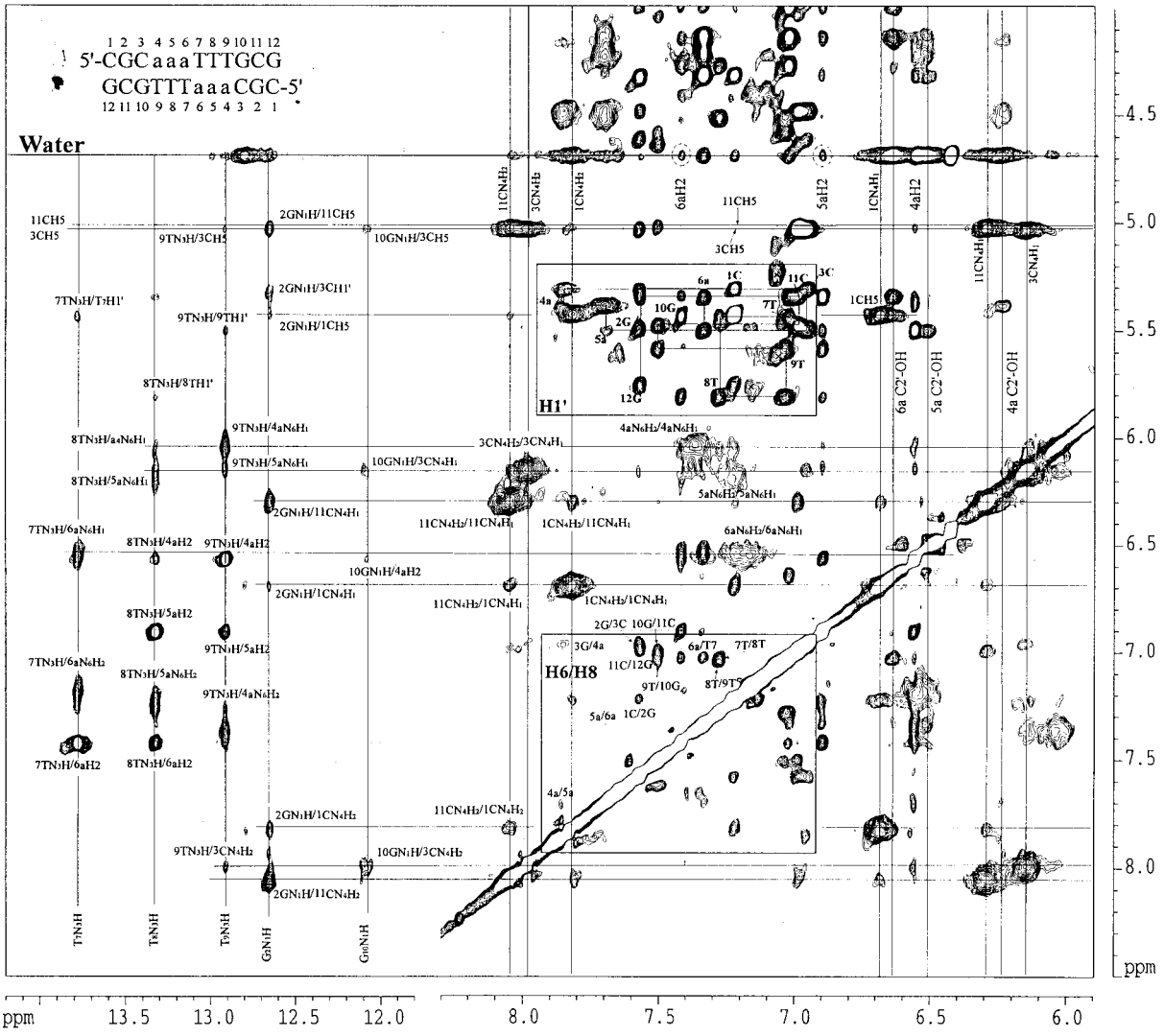

Figure 1. Expansion of the 100 ms water NOESY spectrum of $[d(CGC)r(aaa)d(TTTGCG)]_2$ at 278 K, 600 MHz. For the imino and amino protons, cross-peaks are labeled according to their assignments. In the base to H1′ region, the intraresidue H6/H8-H1′ cross-peaks are labeled with their residue numbers. Two broken-line circles show the hydration cross-peaks of H2 protons of 5a and 6a, while 4a H2 is buried under the C2′-OH cross-peaks. Three C2′-hydroxyl protons are labeled according to their chemical shifts.

The exchangeable imino and amino protons were assigned explicitly by the well-established procedure except for the amino protons of guanosines (Figure 1). The amino protons of guanosines could hardly be observed in normal Watson-Crick base-pairing due to the extreme broadening (>100 Hz) caused by rotation of the amino group around the C-N bond (Mueller *et al.*, 1995). In addition, we have observed three sets of NOEs from the three labile protons resonate at 6.2 ~ 6.6 ppm to the ribose protons. The distances between 2G, 10G, and 12G amino protons to 4a, 5a, and 6a ribose H2′ protons are too long to have NOEs. Since the amino and imino protons of the bases have been assigned, we are left with the only remaining possibility being that the three slowly exchanging labile protons at 6.2 ~ 6.6 ppm (Figure 1) must belong to RNA 2′OH hydroxyl groups. Extra support for these assignments follows from the presence of cross-peaks with the RNA H1′ and H2′ protons and even the H3′, H4′, H5′/H5″ protons (see Figure 3). These labile protons do not give rise to any detectable NOEs to any imino protons, which is consistent with their assignments as ribose 2′OH protons. Their chemical shifts (6.2 ~ 6.6 ppm) are in agreement with previously published assignments of ribose hydroxyl protons (Fedoroff *et al.*, 1997; Conte *et al.*, 1996; Leroy *et al.*, 1985).

Comparison of the 1D cross-sections of NOESY and ROESY spectra at the water chemical shift along the *F*2 dimension provides evidence for hydration (Figure 2). It is important to note that coincident chemical shifts, especially H3′ and H4′ protons of nucleic acids, can give cross-peaks along the water chemical shift. This coincidence can be ruled out by performing experiments at different temperatures, which give different water chemical shifts to confirm the water signals. For long-lived water molecules (correlation time $\tau_c > 0.3$ ns), with opposite signs of NOE and ROE, cross-peaks were found to all H2 and H1′ protons of the RNA adenine bases, except for 4a H2, which was buried under the intense hydroxyl signals at 6.1-6.7 ppm. Similar water-H1′ cross-peaks in RNA were observed previously (Conte *et al.*, 1996). In contrast, cross-peaks to the H1′ protons are usually not detected in DNA, except at the ends of the duplex or at much longer mixing times. These water-H1′ peaks could arise from several possible mechanisms. First, there could be long-lived water molecules around the H1′ proton close enough to cause positive NOE peaks. Second, there could be a rapid exchange between the RNA C2′-OH and water molecules such that the magnetization was relayed to the H1′ proton. Cross-peaks between RNA adenine H1′ and hydroxyl groups observed in the NOESY spectrum (Figure 1) further confirmed the spatial relation of H1′ and hydroxyl protons.

The methyl group of 7T exhibited a positive NOE to water at 278 K (Figure 2), i.e. with a water

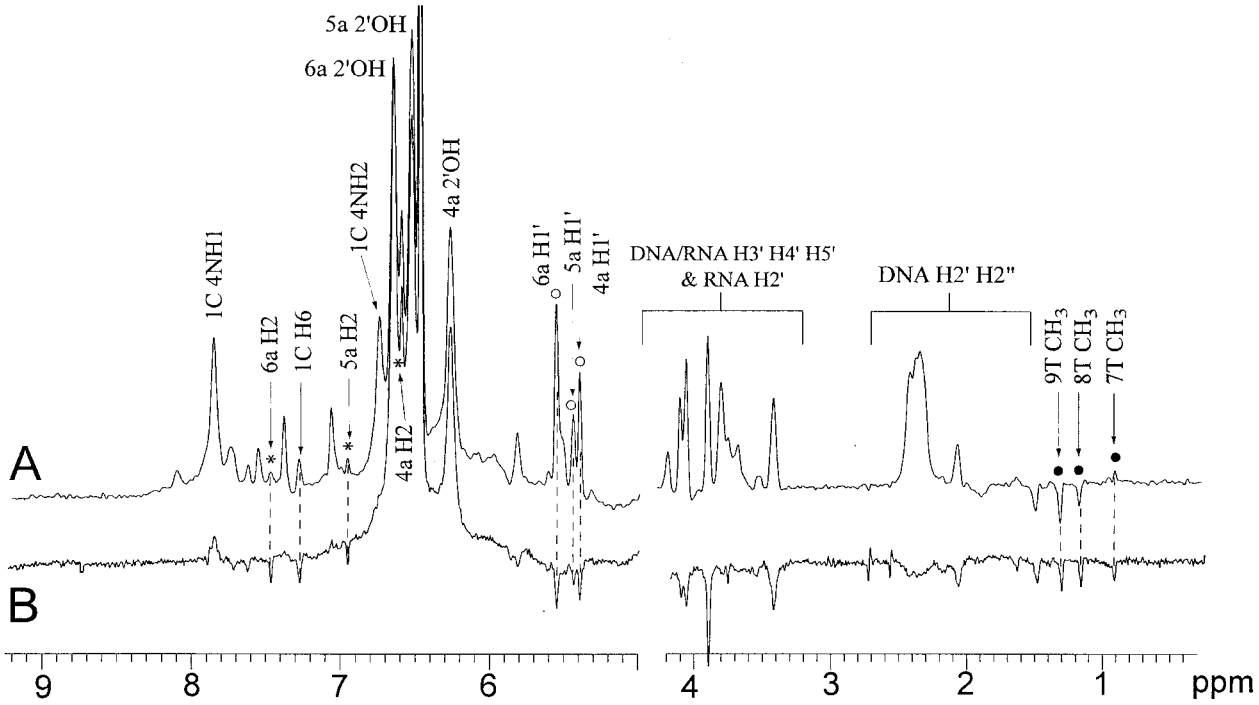

Figure 2. Cross-sections through the water chemical shift along the *F*1 dimension of $[d(CGC)r(aaa)d(TTTGCG)]_2$ at 278 K, 600 MHz. (a) NOESY (mixing time = 100 ms). (b) ROESY (mixing time = 50 ms). The hydration peaks of adenine H2 and H1′ protons are labeled with asterisks (*) and open circles (○) respectively. The hydration peaks of thymine methyl protons are labeled with filled circles (●).

correlation time longer than 0.3 ns, then changed its sign to a negative NOE when the temperature was raised to 300 K (data not shown). However, NOE peaks of the other two methyl groups (8T and 9T), more distant from the center of the duplex, were negative at all temperatures. Such a positive NOE peak to water from the 7T methyl group was not observed in pure DNA duplexes (Jacobson *et al*., 1996; Liepinsh *et al*., 1992, 1994; Sunnerhagen *et al*., 1998). Different signs of the NOE cross-peaks to water of the three neighboring thymine bases may imply two structural features. First, the rapid rotation of the methyl groups was restricted due to a narrower groove width or a shallower groove depth in the central region (7T). Second, the extra hydroxyl group of the preceding 6a in the same strand contributed extra relayed magnetization by exchange with water through the hydroxyl proton, while the interstrand interactions with 8T and 9T were too weak to make a significant contribution. In both cases, water molecules were relatively more accessible to the methyl group of 7T rather than 8T or 9T. One thing that should be pointed out is, based on our unpublished structural studies, only DNA residue 7T in the RNA-DNA junction adopts an O4′-*endo* sugar conformation (intermediate between *B*-form and *A*-form). The other DNA residues, including residue 3C in the DNA-RNA junction, adopt C1′-*exo* or C2′-*endo* conformations (*B*-form).

We also measured the bound water correlation time quantitatively using the ratio of NOESY and ROESY cross-peak volumes (equations (3) and (4)) (Lane *et al*., 1997). The bound water correlation time for 5a H2 was found to be 0.34-0.57 ns ($R = -0.14(\pm 0.11)$) and for 6a H2 was found to be 0.33-0.39 ns ($R = -0.08(\pm 0.04)$) at 283 K. These values are similar to those found in its DNA (Lane *et al*., 1997) and RNA (Conte *et al*., 1996) analogs. It is important to note that, because the correlation time curve for bound water can change sign when τ_c is near 0.3 ns, extra caution must be taken to prevent baseline distortion in processing NOESY and ROESY spectra.

Orientation and exchange rate of C2′-hydroxyl protons

Molecular modeling studies of the RNA duplexes and the DNA·RNA hybrids show that there are three stable rotamers for the RNA C2′-OH hydroxyl groups (Auffinger & Westhof, 1997). In these rotamers, the C2′-OH can hydrogen bond to O3′ of the 3′-phosphate group ($\phi = 90^\circ$, when the C2′-OH-H1′ distance is large, ~3.5 Å, and $^3J_{H2'\text{-}C2'\text{-}OH} < 4$ Hz), to the O4′ of either the neighboring 3′-ribose or in the same sugar ($\phi = 180^\circ$, when the C2′-OH-H1′ distance is short, <2.5 Å, and $^3J_{H2'\text{-}C2'\text{-}OH} = 10\text{-}12$ Hz), or toward the attached base ($\phi = 0$ to -30°, when the C2′-OH-H1′ distance < 2.5 Å, and $J_{H2'\text{-}C2'\text{-}OH} = 4\text{-}7$ Hz) (Gyi *et al*., 1998a,b). Among these orientations, the O3′ direction is the most favorable for the hydrogen bonding framework (Auffinger & Westhof, 1997). As we can see from Figure 1, the observed 4a 2′OH-H1′, 5a 2′OH-H1′, and 6a 2′OH-H1′ NOE distances are all close to or even larger than 3.5 Å using the cytosine H5-H6 distance (2.5 Å) as a standard. Thus, all of the three RNA C2′-OH groups tend to orient toward the O3′ direction and hence the small $^3J_{H2'\text{-}C2'\text{-}OH}$ values. This was further confirmed by the correlation spectroscopy studies. We did not observe any cross-peak of the three RNA 2′OH protons from TOCSY (mixing times of 20 ms, 46 ms, 200 ms, 500 ms at pH 5.5-7.5, 273 K and 278 K) and HMBC (pH 7.0, 273 K) spectra due to the possible O3′ domain conformation ($^3J_{H2'\text{-}C2'\text{-}OH} < 4$ Hz). However, we did observe the intensity modulations of ribose protons (H2′, H2″, H3′ and H4′) due to the TOCSY mixing times.

On the other hand, many cross-peaks were detected along the C2′-OH chemical shift in the NOESY spectrum recorded at 273 K (Figure 3). There were more and stronger cross-peaks along the chemical shift of 6a C2′-OH than those of 5a and 4a, which in turn had few weak cross-peaks. Presumably, the hydration pattern and geometry of the grooves, especially the minor groove in the hybrid segment may be the cause of this trend. The 6a C2′-OH showed stronger intra-residue cross-peaks with H3′ and H1′ and one weaker cross-peak with H8 of the base, but there were no observable cross-peaks with H5′/H5″. The H4′ chemical shifts of 5a, 6a and 7T were very close and it was difficult to identify unambiguously the C2′-OH to H4′ cross-peaks in this region. However, there were two inter-residue cross-peaks between 6a C2′-OH and the following 7T H5′/H5″ and H6 protons. When the orientation of C2′-OH is toward O3′ of the 3′phosphate group, the distances of C2′-$OH_{(i)}$ to $H3'_{(i)}$, $H1'_{(i)}$, $H5'_{(i+1)}$ and $H8/H6_{(i+1)}$ are shorter than those of C2′-OH to $H4'_{(i)}$ and $H8/H6_{(i)}$. Since we have also observed a distinct hydration pattern in the center of the hybrid segment (i.e. a water correlation time was observed longer than 0.3 ns at the 7T methyl group but not 8T and 9T methyl groups, which are more distant from the center of the duplex), there may be long-lived water molecules between 5a and 6a 2′OH protons to mediate stronger NOEs to the ribose protons. Although the possibility of existing multiple rotamers cannot be ruled out for 2′OH groups, the O3′ orientation is still the most preferred compared with O4′ and base orientations in $[d(CGC)r(aaa)d(TTTGCG)]_2$ due to the large distances between 2′OH and H1′ protons.

The exchange rate of the C2′-hydroxyl protons with solvent water was obtained from measurement of the linewidth of the hydroxyl proton cross-peaks in NOESY spectra along the water chemical shift in the *F*2 dimension. The linewidth is a sum of many factors (Gyi *et al*., 1998a):

$$L = L_0 + L(\Delta B) + \Sigma J + k/\pi \qquad (5)$$

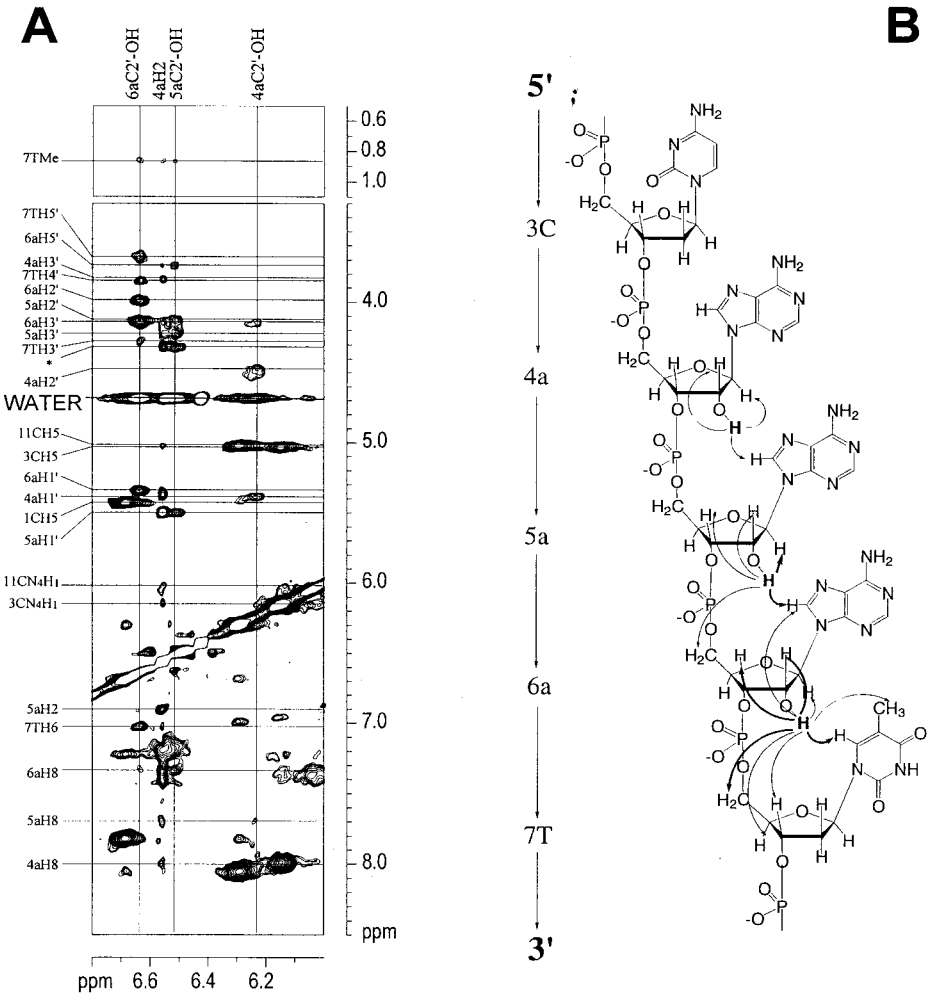

Figure 3. RNA C2′-hydroxyl proton interactions. (a) Expansion of the C2′-OH to all regions of the 100 ms water NOESY spectrum of $[d(CGC)r(aaa)d(TTTGCG)]_2$ at 273 K, 600 MHz. Each chemical shift is labeled on the left with a continuous line along the *F*1 dimension. One ambiguous chemical shift is labeled with an asterisk (*). The chemical shift of 7T H4′ is overlapped with the chemical shifts of 3C H4′ and 9T H4′; however, 3C and 9T H4′ protons are too distant to interact with 6a C2′-hydroxyl proton. Therefore, we labeled this chemical shift as 7T H4′. (b) A representation of the intrastrand DNA·RNA hybrid segment with NOE connectivities. Bold arrows indicate strong NOEs and thin arrows indicate weak NOEs. There are nine intra- and inter-residue NOEs in 6a, but only five and three NOEs in 5a and 4a.

where L_0 is the intrinsic linewidth, $L(\Delta B)$ is the contribution of magnetic field heterogeneity and instrument artifacts and ΣJ is the contribution of unsolved scalar coupling. Subtraction of these factors gives an upper limit estimation of the exchange rate k. It is to be noted that this estimation neglects the fast intermediate rotating motion. As the C2′-OH peaks were partially overlapped, we first did decomposition for overlapping to obtain individual line-widths by assuming that all peaks had Lorentzian line-shapes (Figure S1 in Supplementary Materials). In some conditions, small peaks were not well separable and we neglected them as representing only a small contribution to the whole line-shape. However, due to overlapping and other unsolved scalar coupling, the decomposed line-widths gave us only an estimate of the upper limit of the exchange rate. By performing analysis at several temperatures ranging from 273 to 288 K, we obtained the C2′-OH exchange rate with an overall range of ~5-20/seconds. This exchange rate was lower than that for other DNA·RNA hybrid duplexes studied previously ($k = 26.7(\pm 13.8)$ s^{-1}, which had an r(gaga) sequence in the central region (Gyi *et al.*, 1998a). Based on our unpublished structural studies using NOE and dihedral angle constraints (Figure S2 in Supplementary Materials), the minor groove width of $[d(CGC)r(aaa)d(TTTGCG)]_2$ is closer to the value of 7.5 Å found for the classical *B*-form DNA duplex but differs from that of the *A*-RNA or *A*-DNA duplex (9-11 Å). The narrow minor groove width of $[d(CGC)r(aaa)d(TTTGCG)]_2$ may trap the water molecules and restrict the dynamic motion

of hydroxyl protons, thus lowering their exchange rate with water molecules.

In conclusion, we have studied the hydration of a DNA·RNA chimeric duplex [d(CGC)r(aaa)-d(TTTGCG)]$_2$, in which the hybrid junctions are flanked by DNA duplexes at both ends. The distinct hydration patterns of the RNA adenine H2 and H1′-OH protons, may provide a molecular basis to further understand the structure and recognition of DNA·RNA hybrid and chimeric duplexes.

Acknowledgments

We thank Dr Moti L. Jain for revising the English for us. This study was carried out on the 600 MHz NMR spectrometer at the Regional Instrument Center at Hsinchu, National Science Council, Taiwan, Republic of China. We thank the National Science Council of the Republic of China for research grants.

References

Arnott, S., Chandrasekaran, R., Millane, R. P. & Park, H.-S. (1986). DNA-RNA hybrid secondary structures. *J. Mol. Biol.* **188**, 631-640.

Auffinger, P. & Westhof, E. (1997). Rules governing the orientation of the 2′-hydroxyl group in RNA. *J. Mol. Biol.* **274**, 54-63.

Ban, C., Ramakrishnan, B. & Sundaralingam, M. (1994a). Crystal structure of the highly distorted chimeric decamer r(C)d(CGGCGCCG)r(G): spermine complex-spermine binding to phosphate only and minor groove tertiary base-pairing. *Nucl. Acids Res.* **22**, 5466-5476.

Ban, C., Ramakrishnan, B. & Sundaralingam, M. (1994b). A single 2′-hydroxyl group converts B-DNA to A-DNA: crystal structure of the DNA-RNA chimeric decamer duplex d(CCGGC)r(G)d(CCGG) with a novel intermolecular G:C base-paired quadruplet. *J. Mol. Biol.* **236**, 275-285.

Berman, H. M. (1994). Hydration of DNA: take 2. *Curr. Opin. Struct. Biol.* **4**, 345-350.

Billeter, M., Guntert, P., Luginbuhl, P. & Wuthrich, K. (1996). Hydration and DNA recognition by homeodomains. *Cell,* **85**, 1057-1065.

Chou, S.-H., Flynn, P. & Reid, B. R. (1989). High resolution NMR study of a synthetic DNA/RNA hybrid dodecamer of pribnow promoter sequence: d(CGTTATAATGCG)r(CGCAUUAUAACG). *Biochemistry,* **28**, 2422-2435.

Chou, S.-H., Flynn, P., Wang, A. & Reid, B. (1991). High-resolution NMR. studies of chimeric DNA-RNA-DNA duplexes, heteronomous base pairing, and continuous base stacking at junctions. *Biochemistry,* **30**, 5248-5257.

Conte, M. R., Conn, G. L., Brown, T. & Lane, A. N. (1996). Hydration of the RNA duplex r(CGCAAAUUUGCG)2 determined by NMR. *Nucl. Acids Res.* **24**, 3693-3699.

Cross, C. W., Rice, J. S. & Gao, X. (1997). Solution structure of an RNA:DNA hybrid duplex containing a 3′-thioformacetal linker and an RNA A-tract. *Biochemistry,* **36**, 4096-4107.

Denisov, V. R., Carlstrom, G., Venu, K. & Halle, B. (1997). Kinetics of DNA hydration. *J. Mol. Biol.* **268**, 118-136.

Drew, H. R. & Dickerson, R. E. (1981). Structure of a *B*-DNA dodecammer. III geometry of hydration. *J. Mol. Biol.* **151**, 535-556.

Egli, M., Usman, N., Zhang, S. & Rich, A. (1992). Crystal structure of an Okazaki fragment at 2 Å resolution. *Proc. Natl Acad. Sci. USA,* **89**, 534-538.

Egli, M., Usman, N. & Rich, A. (1993). Conformational influence of the ribose 2′-hydroxyl group: crystal structures of DNA-RNA chimeric duplexes. *Biochemistry,* **32**, 3221-3237.

Fawthrop, S. A., Yang, J.-C. & Fisher, J. (1993). Structural and dynamic studies of a non-self complementary dodecamer DNA duplex. *Nucl. Acids Res.* **21**, 4860-4866.

Fedoroff, O. Y., Salazar, M. & Reid, B. R. (1993). Structure of a DNA:RNA hybrid duplex: why RNase H does not cleave pure DNA. *J. Mol. Biol.* **233**, 509-523.

Fedoroff, O. Y., Salazar, M. & Reid, B. R. (1996). Structural variation among retroviral primer-DNA junctions: solution structure of the HIV-1 (−)-strand Okazaki Fragment r(gcca)d(CTGC)/d(GCAGTGGC). *Biochemistry,* **35**, 11070-11080.

Fedoroff, O. Y., Ge, Y. & Reid, B. R. (1997). Solution structure of r(gaggacug): d(CAGTCCTC) hybrid: implications for the initiation of HIV-1 (+)-strand synthesis. *J. Mol. Biol.* **269**, 225-239.

Gao, X. & Jeffs, P. W. (1994). Sequence-dependent conformational heterogeneity of a hybrid DNA:RNA dodecamer duplex. *J. Biomol. NMR,* **4**, 367-384.

Gmeiner, W. H., Rao, K. E., Rayner, B., Vasscur, J.-J., Morvan, F., Imbach, J.-L. & Lown, J. W. (1990). Polarity of annealing and structural analysis of the RNase H resistant a-5′-d[TACACA]:b-5′r[AUGUGU] hybrid determined by high-field ^{1}H, ^{13}C, and ^{31}P NMR analysis. *Biochemistry,* **29**, 10329-10341.

Gonzalez, C., Stec, W., Kobylanska, A., Hogrefe, R. I., Reynolds, M. & James, T. L. (1994). Structural study of a DNA:RNA hybrid duplex with a chiral phosphorothioate moiety by NMR: extraction of distance and torsion angle constraints and imino proton exchange rates. *Biochemistry,* **33**, 11062-11072.

Gonzalez, C., Stec, W., Reynolds, M. A. & James, T. L. (1995). Structure and dynamics of a DNA:RNA hybrid duplex with a chiral phosphorothioate moiety: NMR and molecular dynamics with conventional and time-averaged restraints. *Biochemistry,* **34**, 4969-4982.

Guerri, A., Simpson, I. J. & Neidle, S. (1998). Visualisation of extensive water ribbons and networks in a DNA minor-groove drug complex. *Nucl. Acids Res.* **26**, 2873-2878.

Gyi, J. I., Conn, G. L., Lane, A. N. & Brown, T. (1996). Comparison of the thermodynamic stabilities and solution conformations of DNA:RNA hybrids containing purine-rich and pyrimidine-rich strands with DNA and RNA duplexes. *Biochemistry,* **35**, 12538-12548.

Gyi, J. I., Lane, A. N., Conn, G. L. & Brown, T. (1998a). The orientation and dynamics of the C2′-OH and hydration of RNA and DNA-RNA hybrids. *Nucl. Acids Res.* **26**, 3104-3110.

Gyi, J. I., Lane, A. N., Conn, G. L. & Brown, T. (1998b). Solution structures of DNA:RNA hybrids with purine-rich and pyrimidine-rich strands: comparison

with the homologous DNA and RNA duplexes. *Biochemistry*, **37**, 73-80.

Hare, D. R., Wemmer, D. E., Chou, S.-H., Drobny, G. & Reid, B. R. (1983). Assignment of the non-exchangeable proton resonances of d(CGCGAATTCGCG) using two-dimensional nuclear magnetic resonance methods. *J. Mol. Biol.* **171**, 319-336.

Hashem, G. M., Pham, L., Vaughan, M. R. & Gray, D. M. (1998). Hybrid oligomer duplexes formed with phosphorothioate DNAs: CD spectra and melting temperatures of S-DNA:RNA hybrids are sequence-dependent but consistent with similar heteronomous conformations. *Biochemistry*, **37**, 61-72.

Jacobson, A., Leupin, W., Liepinsh, E. & Otting, G. (1996). Minor groove hydration of DNA in aqueous solution: sequence-dependent next neighbor effect of the hydration lifetimes in d(TTAA)2 segments measured by NMR spectroscopy. *Nucl. Acids Res.* **24**, 2911-2918.

Jaishree, T. N., van der Marel, G. A., van Boom, J. H. & Wang, A. H. J. (1993). Structural influence of RNA incorporation in DNA: quantitative nuclear magnetic resonance refinement of d(CG)r(CG)d(CG) and d(CG)r(C)d(TAGCG). *Biochemistry*, **32**, 4903-4911.

Johannesson, H. & Halle, B. (1998). Minor groove hydration of DNA in solution: dependence on base composition and sequence. *J. Am. Chem. Soc.* **120**, 6859-6870.

Katahira, M., Lee, S. J., Kobayashi, Y., Sugeta, H., Kyogoku, Y., Iwai, S., Ohtsuka, E., Benevides, J. M. & Thomas, G. J. J. (1990). Structure in solution of the RNA-DNA hybrid (rA)8(dT)8 determined by NMR and raman spectroscopy. *J. Am. Chem. Soc.* **112**, 4508-4512.

Kubinec, M. G. & Wemmer, D. E. (1992). NMR evidence for DNA bound water in solution. *J. Am. Chem. Soc.* **114**, 8739-8740.

Lane, A. N., Ebel, S. & Brown, T. (1993). NMR assignments and solution conformation of the DNA:RNA hybrid duplex d(GTGAACTT):r(AAGUUCAC). *Eur. J. Biochem.* **215**, 297-306.

Lane, A. N., Jenkins, T. C. & Frenkiel, T. A. (1997). Hydration and solution structure of d(CGCAAATTTGCG)2 and its complex with propamidine from NMR and molecular modelling. *Biochim. Biophys. Acta*, **1350**, 205-220.

Leroy, J. L., Broseta, D. & Gueron, M. (1985). Proton exchange and base-pair kinetics of poly(rA)·poly(rU) and poly(rI)·poly(rC). *J. Mol. Biol.* **184**, 165-178.

Liepinsh, E., Otting, G. & Wuthrich, K. (1992). NMR observation of individual molecules of hydration water bound to DNA duplexes: direct evidence for a spine of hydration water present in aqueous solution. *Nucl. Acids Res.* **20**, 6549-6553.

Liepinsh, E., Leupin, W. & Otting, G. (1994). Hydration of DNA in aqueous solution: NMR evidence for a kinetic destabilization of the minor groove hydration of d-(TTAA)2 versus d-(AATT)2 segments. *Nucl. Acids Res.* **22**, 2249-2254.

Maltseva, T. V., Agback, P., Repkova, M. N., Venyaminova, A. G., Ivanova, E. M., Sandstrom, A., Zarytova, V. F. & Chattopadhyaya, J. (1994). The solution structure of a 3′-phenazinium. (Pzn) tethered DNA-RNA duplex with a dangling adenosine: r(5′GALTUGAA3′):d(5′TCAATC3′-Pzn). *Nucl. Acids Res.* **22**, 5590-5599.

Morton, C. J. & Ladbury, J. E. (1996). Water mediated protein-DNA interactions: the relationship of thermodynamics to structural detail. *Protein Sci.* **5**, 2115-2118.

Mueller, L., Legault, P. & Pardi, A. (1995). Improved RNA structure determination by detection of NOE contacts to exchange-broadened amino protons. *J. Am. Chem. Soc.* **117**, 11043-11048.

Mujeeb, A., Reynolds, M. A. & James, T. L. (1997). High-resolution NMR of an antisense DNA:RNA hybrid containing alternating chirally pure Rp methylphosphonates in the DNA backbone. *Biochemistry*, **36**, 2371-2379.

Nishizaki, T., Iwai, S., Ohkubo, T., Kojima, C., Nakamura, H., Kyogoku, Y. & Ohtsuka, E. (1996). Solution structures of DNA duplexes containing a DNA:RNA hybrid region, d(GG)r(AGAU)d(GAC):d(GTCATCTCC) and d(GGAGA)r(UGAC):d(GTCATCTCC). *Biochemistry*, **35**, 4016-4025.

Otting, G., Liepinsh, E. & Wuthrich, K. (1991). Protein hydration in aqueous solution. *Science*, **54**, 974-980.

Phan, A. T., Leroy, J. L. & Gueron, M. (1999). Determination of the residence time of water molecules hydrating *B*′-DNA and *B*-DNA, by one-dimensional zero-enhancement nuclear Overhauser effect spectroscopy. *J. Mol. Biol.* **286**, 505-519.

Piotto, M., Saudek, V. & Sklenar, V. (1992). Gradient-tailored excitation for single-quantum NMR spectroscopy of aqueous solutions. *J. Biomol. NMR*, **2**, 661-665.

Prive, G. G., Heinemann, U., Chandrasegaran, S., Kan, L. S., Kopka, M. L. & Dickerson, R. E. (1987). Helix geometry, hydration, and GA mismatch in a *B*-DNA decamer. *Science*, **238**, 498-504.

Quintana, J. R., Grzeskowiak, K., Yanagi, K. & Dickerson, R. E. (1992). Structure of a *B*-DNA decamer with a central TA step: CGATTAATCG. *J. Mol. Biol.* **225**, 379-395.

Rice, J. & Gao, X. (1997). Conformation of formacetal and 3′-thioformacetal nucleotide linkers and stability of their antisense RNA:DNA hybrid duplexes. *Biochemistry*, **36**, 399-411.

Saenger, W. (1984). *Principles of Nucleic Acid Structure*, Springer, New York.

Salazar, M., Champoux, J. J. & Reid, B. R. (1993a). Sugar conformations at hybrid duplex junctions in HIV-1 and Okazaki fragments. *Biochemistry*, **32**, 739-744.

Salazar, M., Fedoroff, O. Y., Miller, J. M., Ribeiro, N. S. & Reid, B. R. (1993b). The DNA strand in DNA:RNA hybrid duplexes is neither *B*-form nor *A*-form in solution. *Biochemistry*, **32**, 4207-4215.

Salazar, M., Fedoroff, O. Y., Zhu, L. & Reid, B. R. (1994). The solution structure of the r(gcg)d(TATACCC):d(GGGTATACGC) Okazaki fragment contains two distinct duplex morphologies connected by a junction. *J. Mol. Biol.* **241**, 440-455.

Salazar, M., Fedoroff, O. Y. & Reid, B. R. (1996). Structure of chimeric duplex junctions: solution conformation of the retroviral Okazaki-like fragment r(ccca)d(AATGA)/d(TCATTTGGG) from moloney murine leukemia virus. *Biochemistry*, **35**, 8126-8135.

Schwabe, J. W. (1997). The role of water in protein-DNA interactions. *Curr. Opin. Struct. Biol.* **7**, 126-134.

Steely, H. T. J., Gray, D. M. & Ratliff, R. L. (1986). CD of homopolymer DNA-RNA hybrid duplexes and triplexes containing AT or AU base pairs. *Nucl. Acids Res.* **14**, 10071-10089.

Sunnerhagen, M., Denisov, V. P., Venu, K., Bonvin, A. M. J. J., Carey, J., Halle, B. & Otting, G. (1998).

Water molecules in DNA recognition 1: hydration lifetimes of trp operator DNA in solution measured by NMR spectroscopy. *J. Mol. Biol.* **282**, 847-858.

Szyperski, T., Gotte, M., Billeter, M., Perola, E., Cellai, L., Heumann, H. & Wuthrich, K. (1999). NMR structure of the chimeric hybrid duplex r(gcaguggc)-r(gcca)d(CTGC) comprising the tRNA-DNA junction formed during initiation of HIV-1 reverse transcription. *J. Biomol. NMR*, **13**, 343-355.

Wang, A. H.-J., Fujii, S., van Boom, J. H., van der Marel, G. A., van Boeckel, S. A. A. & Rich, A. (1982). Molecular structure of r(GCG)d(TATACGC): a DNA-RNA hybrid helix joined to double helical DNA. *Nature*, **299**, 601-604.

Wuthrich, K. (1986). *NMR of Proteins and Nucleic Acids*, John Wiley & Sons, New York, USA.

Zhou, D. & Bryant, R. G. (1996). Water molecule binding and lifetimes on the DNA duplex d(CGCGAATTCGCG)2. *J. Biomol. NMR*, **8**, 77-86.

Zhu, L., Salazar, M. & Reid, B. R. (1995). DNA duplexes flanked by hybrid duplexes: the solution structure of chimeric junctions in [r(cgcg)d(TATACGCG)]2. *Biochemistry*, **34**, 2372-2380.

Edited by I. Tinoco

(Received 5 August 1999; received in revised form 7 November 1999; accepted 16 November 1999)

http://www.academicpress.com/jmb

Supplementary Material comprising two Figures is available from JMB Online.